Journal of Applied Sciences

ISSN 1812-5654

science alert

ANSInet
an open access publisher
http://ansinet.com

Journal of Applied Sciences 7 (4): 547-552, 2007
ISSN 1812-5654

2D Detached-Eddy Simulation Around Elliptic Airfoil at High Reynolds Number

[1]A. Benazza, [2]E. Blanco and [3]M. Abidat
[1]Départment of Mechanical Engineering, University of Sidi Bel Abbès, PB 89, 22000 Algeria
[2]Universidad de Oviedo, Dpto. de Energía. Campus de Viesques, 33271-Gijón, Spain
[3]Laboratoire de Mécanique Appliquée, Faculté de Génie Mécanique,
USTOran, BP 1505, Oran Algeria

Abstract: A simulation of the flow field around an elliptic profile were performed using a finite volume method at chord Reynolds number of 7.21×10^6. The solutions were computed over a hybrid mesh using a Detached Eddy Simulation approach and the Spallart-Allmaras (S-A) turbulence model. Lift and drag coefficients (C_l and C_d) were computed from zero lift to angles above stall. The influence of RANS zone size on the DES predictions was investigated. The accuracy of DES predictions is superior to that of S-A model and the computed values of C_l and C_d are in good agreement with experimental data up to stall point. The complex shedding process and forces modulation appears to be represented reasonably at least in relation to adequate value of Strouhal number (St = 0.25) for this Reynolds number. This 2D DES study fails to correctly predict the stall for this configuration of flow. Prediction of separation at stall continues to strongly challenge the current DES modeling approach.

Key words: Detached-eddy simulation, lift, drag, stall, vortex shedding

INTRODUCTION

Elliptic profile provides a canonical flow behaviour characteristic of typical engineering flow configurations that include adverse pressure, streamline curvature and boundary layer separation. On the other hand, these symmetric airfoils are generally used in axial reversible jet fans and some vertical wind turbines. In such flows, parameters such as angle of attack and Reynolds number can greatly influence the nature of separation and the unsteady wake structure. Current engineering approaches for unsteady flows prediction rely primarily on the Reynolds-Averaged Navier-Stockes (RANS) equations. While the most popular RANS models appear to yield predictions of comparable accuracy in attached flows and as well as those with shallow separations, it does not appear that RANS turbulence models are sufficiently accurate for reliable prediction of inherently unsteady flows. Techniques such as Large Eddy Simulation (LES) are attractive for flows regime with significant effects of separation. The uncertainty of the modelling is reduced when the large energy-containing scales of motion are resolved. When applied to boundary layers, however, the computational cost of whole-domain LES does not differ significantly from that of Direct Numerical Simulation (Spallart *et al*., 1997).

The above considerations motivate development of hybrid strategies that combine within a single simulation both LES and RANS. Detached Eddy Simulation is among the actively applied hybrid RANS-LES strategies. The method aims at entrusting the boundary layer to RANS while the detached-eddies in separated regions are resolved using LES.

The DES approach has proven to be especially effective for prediction of massively separated flows (Constantinescu *et al*., 2002; Viswanathan *et al*., 2003) in turn motivating extension of the method to the accurate prediction of flows exhibiting shallow separation, either unclosed or a bubble.

As the cylinder and the sphere, the ellipse belongs to the class of separated flows for which the location of flow detachment is not fixed by the geometry. Unlike geometries that fix separation lines, such as occurs over a square cylinder, prediction of smooth-surface separation stresses the capacity of the model for predicting the location of flow detachment.

In natural applications of DES the entire boundary layer is treated by the RANS model and the detached regions away from the wall are handled by an LES model. There is a trend, at least in fundamental studies, to predict parts of boundary layers with LES (Nikitin *et al*., 2000). This motivates extension of method to investigate the influence of RANS zone size on the DES predictions.

Corresponding Author: A. Benazza, Départment of Mechanical Engineering, University of Sidi Bel Abbès, PB 89, 22000 Algeria
Fax: 00213 48 56 41 00

In literature few studies of flow over elliptic profile have been performed. Lugt and Haussling (1974) have studied the flow over thin ellipses at various angles of attack for low Reynolds number. Mittal and Balachandar (1996) have performed Direct Numerical Simulation of 2D and 3D flows at low Reynolds numbers. They found that the values of Strouhal number agree well with experimental values of St for flows over circular cylinders at the same Reynolds numbers. William and Brown (1937) have tested an elliptic cylinder over range of Reynolds number from 0.3×10^6 to 7.21×10^6. Lift, drag and pitching moment were measured from zero lift to angles above stall. The values of C_l and C_d are given for the model of aspect ratio 6 as tested, corrected for wind tunnel interference and for infinite aspect ratio, using the usual aerofoil formulae.

In this study a simulation of incompressible flow over an elliptic airfoil of aspect ratio 6 was performed using 2D DES model. For massively separated flows, full 3-D simulations are required, even for nominally two (2-D) geometries. The simulation of (3-D) unsteady flow is a computationally intensive task compared to 2D treatment. In addition the results from the work by Travin *et al.* (2000) show that the 2D DES is closer to 3D DES in turbulent separation cases than in the laminar separation cases. The predicted values of drag and lift coefficients are compared to experimental results of William and Brown (1937) and to those obtained from RANS simulations using S-A model (Benazza *et al.*, 2005).

FLOW DESCRIPTION AND COMPUTATIONAL METHOD

The specific flow of interest is that over an elliptic airfoil at Reynolds number of 7.21×10^6 and Mach number of 0.07. The general characteristics of flow are illustrated in Fig. 1. The flow is evidently separated from the round trailing end and the two separation points move, together with the wake, steadily around the end from the pressure towards the suction side, as the angle of attack is increased. At high Reynolds number, it is assumed that the transition occurred at small value of x/C very close to leading edge and that conditions are favorable for a study of a turbulent boundary layer of considerable length.

The governing equations for two-dimensional viscous incompressible flow in Cartesian coordinates can be expressed as:

$$\frac{\partial u_i}{\partial x_i} = 0 \tag{1}$$

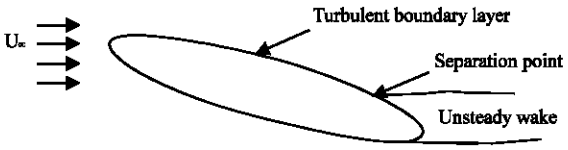

Fig. 1: Flow configuration around ellipse

$$\rho\left(\frac{\partial u_i}{\partial t}+u_j\frac{\partial u_i}{\partial x_j}\right)=-\frac{\partial p}{\partial x_j}+\mu\Delta u_i+\rho g_i \tag{2}$$

Turbulence model: The DES approach used is based on the Spalart-Allmaras turbulence model (Spalart and Allmaras, 1994). To obtain the model used in the DES formulation, the length scale of the S-A destruction term is modified to be the minimum of the distance to the closest wall and a length scale proportional to the local grid spacing.

$$\tilde{d} = \min(d, C_{DES}\Delta) \tag{3}$$

Where, Δ is the largest distance between the cell center under consideration and the cell center of the nearest neighbors and C_{DES} is a model constant. Near the wall, where $\tilde{d}$ = d the model works as a standard S-A turbulence model. In the regions, far from the wall, where $d>C_{DES}\Delta$ the length scale of model becomes grid-dependent and the closure is a one equation model for the subgrid-scale (SGS) eddy viscosity. When the production and the destruction terms are balanced, this model reduces to an algebraic mixing length Smargorinsky-like subgrid model $(\tilde{V}\alpha S\Delta^2)$. The additional model constant C_{DES} = 0.65 was set in homogeneous turbulence.

Numerical method: The governing equations are solved by a cell centered finite volume approach using the fluent code. The grid arrangement is collocated and the Rhie and Chow interpolation method (Rhie and Chow, 1983) is used to prevent the checker boarding of pressure. In LES (DES) model most of the numerical procedures are based on central differencing scheme (CDS), because of its non-dissipative and energy-conserving properties. Upwind schemes are unsuitable because of their overly diffusive nature. At high Reynolds number, it is well known that CDS can produce unbounded solutions and non physical wiggles. In LES, the situation is exacerbated by usually very low sub-grid-scale turbulent diffusivity. To overcome these stability problems the convective flux in momentum equations is computed by means of the bounded central differencing scheme. The bounded CDS scheme is a composite normalized variable diagram (NVD)

scheme that consists of a pure central differencing, a blended scheme of the central differencing and the second order upwind scheme.

A Green-Gauss reconstruction of the gradient is used for all gradients calculations used to discretize the convection and diffusion terms of the transport equations. The time discretization is performed by a second order implicit scheme. Second order time stepping is an established technique for improving the time accuracy of conventional numerical schemes for unsteady flow computations. A point wise-implicit Gauss-Seidel scheme is employed for advancement of the discretized system.

Boundary conditions: At the inflow boundary the instantaneous velocity normal to boundary is simply set to its mean velocity counterpart. This option is suitable when the level of turbulence at inflow boundary is negligible or does not play a mayor role in the accuracy of the overall solution. The value of subgrid scale eddy viscosity is set to low level: ($\mu_{SGS}/\mu = 1$). No slip velocity boundary condition is used at the wall and the turbulent viscosity is set to zero. A Neumann boundary condition for the pressure is applied at the outflow boundary.

Computations tests and grid: The 2D computations were performed using an unstructured grid with hybrid quadrilateral-triangular cells. The quadrilaterals elements were clustered in the near wall region and the first wall normal spacing in a dimensional form was about $y^+ <1$ (Fig. 2). The use of quadrilaterals elements in boundary layer allows using a small wall normal spacing Δy and a large wall parallel spacing Δx, which determine the extension of RANS zone.

There are positive attributes of unstructured grids that relevant to DES. It is possible, for example, to concentrate points in region of interest the focus region introduced in the Young Person's Guide to Detached Eddy Simulation Grids (Spalart, 2001). The YPG defines the average cell size Δ_0 in the focus region as the principal measure of spatial resolution in a DES and assumes that the time step chosen for accuracy, not stability, can be approximate by $\Delta t = \Delta_0/U_{max}$. Assuming a maximum velocity U_{max} in the focus region equal to twice the freestream velocity (U_0), the time step was estimated to $\Delta t = 0.006C/U_0$ where C is the chord length. The iterations number was adjusted to N = 15 in each time step to reduce the residual below an acceptable value.

In the first computation we studied the influence of the RANS zone size d_R ($d_R = C_{DES}\Delta$) on the DES predictions at two angles of attack. Six values of d_R were used corresponding to six different grid sizes generated

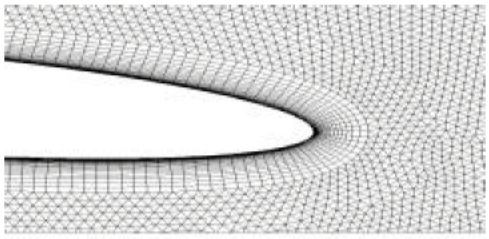

Fig. 2: View of grid in vicinity of the elliptic profile

Table 1: Grids details

Case	Cells	N	Δ_0/C
C1	124508	444	0.0050
C2	106420	316	0.0074
C3	97172	252	0.010
C4	91846	204	0.012
C5	83432	172	0.015
C6	70432	116	0.022

by varying the wall parallel spacing on airfoil and applying the same normal spacing (Table 1). The simulations were performed in a cluster of eight Hydra (2.7 GHz) nodes. The lift and drag coefficients are computed for angles of attack: $\alpha = 10.5$ and $\alpha = 17.5$ and are compared with available experimental results.

In the second part of this study we have used a grid of 91846 cells which have given best results in the first computation. The Simulations of 2D incompressible flow were performed from low angles of attack to angles above the stall for a chord Reynolds number of 7.21×10^6.

RESULTS AND DISCUSSION

Figure 3 presents the variations of the relative RANS zone size for the six grids tested. Where Δ is the boundary layer thickness at the station x/C = 0.5 on the pressure side of airfoil. The high values of Δ_0 corresponds to RANS zone of DES that extends in great part of boundary layer, while for the low values of Δ_0, the RANS zone are in order of inner region of boundary layer, as illustrated in Fig. 3.

In Fig. 4 and 5 contours of the instantaneous vorticity magnitude for the two cases C1 and C6 are shown. Figure 4 shows that some eddy content is captured close the wall near the trailing edge and coherent structures appear in the wake, yielding unsteady fluctuations of the lift and drag coefficients. Figure 5 yields marked changes in the flow structure, with a total lack of vortices in all boundary layer and the wake. The DES predictions for this case (C6) tend to steady solution like S-A RANS computation, giving constant values of lift and drag coefficients. The RANS zone size is relatively large and so globally the entire boundary layer is handled

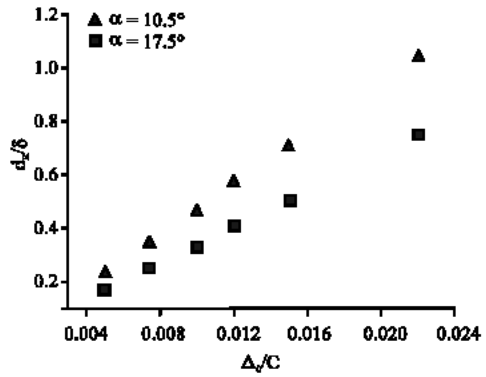

Fig. 3: RANS zone size versus Δ_0/C at x/C = 0.5 on the pressure side of airfoil

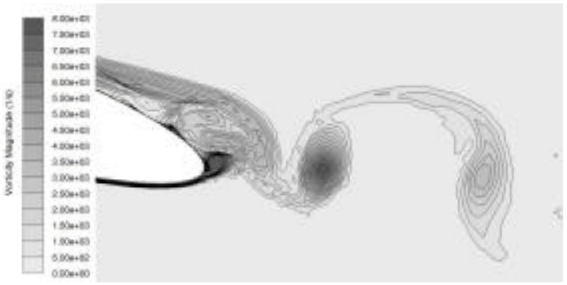

Fig. 4: Contours of the instantaneous vorticity magnitude for case C1 (N = 124508 cells)

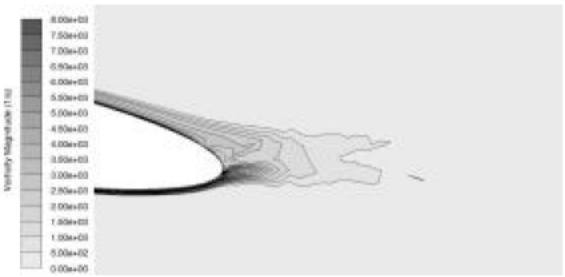

Fig. 5: Contours of the instantaneous vorticity magnitude for case C6 (N = 70432 cells)

by the S-A model. We can say that the RANS zone size influences substantially the prediction of the unsteady features of the flow.

Figure 6 presents the variation of the lift coefficient as a function of the average cell size Δ_0 for different grids. Figure 6 shows that at high values of Δ_0 the predicted lift coefficients differ significantly from those of experimental data. This corresponds to case of large

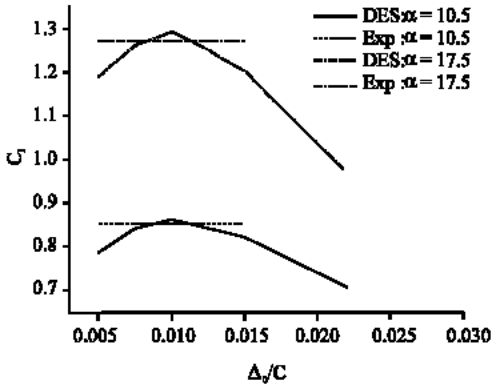

Fig. 6: Lift coefficient for different grids as a function of the average cell size Δ_0/C

RANS zone, as cited above; the predictions tend to steady solution. At low values of Δ_0 the results of lift coefficients are underpredicted. As reported by Kotapati-Apparao *et al.* (2004), as the grid spacing in the wall-parallel directions becomes smaller than about half of the boundary layer thickness, the DES limiter reduces the eddy viscosity below its RANS level and this process can degrades predictions if mesh densities are insufficient to support eddy content in this zone of boundary layer. Both in two cases (α = 10.5° and α = 17.5°) studied the intermediate values of Δ_0 allow to obtain accurate predictions of lift coefficients. Other case was tested using a relatively fine grid of 206300 cells that allows to extent a LES treatment in the great part of logarithm region of boundary layer. The results have shown that some vortices have been captured but the solution presented a large instability due probably to poor prediction of all large scales in inner region using an insufficient mesh density for the LES model. It appears that for the success of DES predictions in such flow, a part of boundary layer must be treated by LES model and RANS zone must extends largely over the logarithm region.

For the second DES test (N = 91846) time averaged drag and lift coefficients are compared with experiment results and with those from S-A predictions in Fig. 7 and 8. At low angles of attack both computed lift and drag coefficients agree well with experimental values for two models. As the angle of attack increases ($10<\alpha<18$), the S-A model overestimates the lift coefficients while DES predictions are in good agreement with experimental results. The differences in the S-A predictions compared to DES predicted values highlight differences in the flow evolution, especially in separation and wake. At 18.45° angle of attack the S-A model predicts separation at x/C = 0.85 and DES predicts boundary layer separation at x/C = 0.80. The S-A

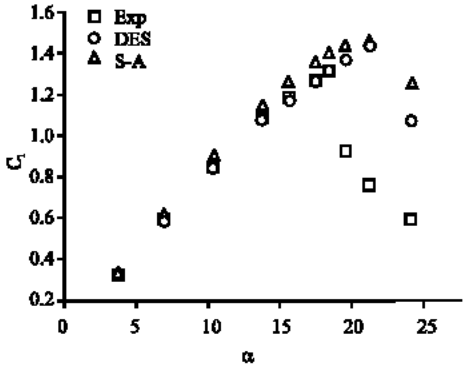

Fig. 7: Variation of lift coefficient with angle of attack

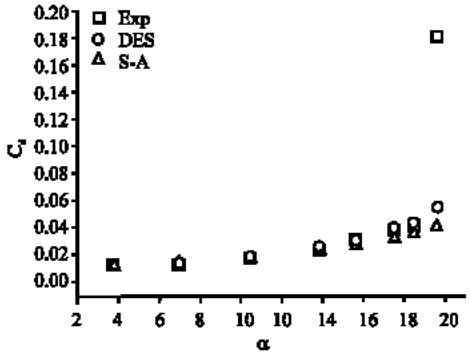

Fig. 8: Drag coefficients versus the angle of attack

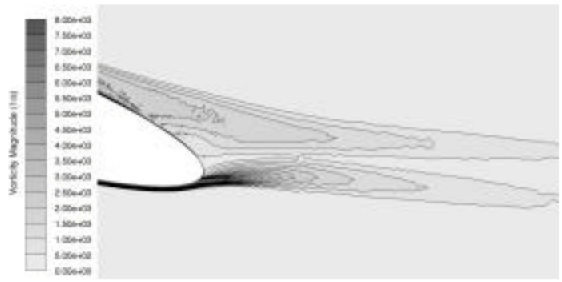

Fig. 9: Contours of vorticity magnitude for S-A model

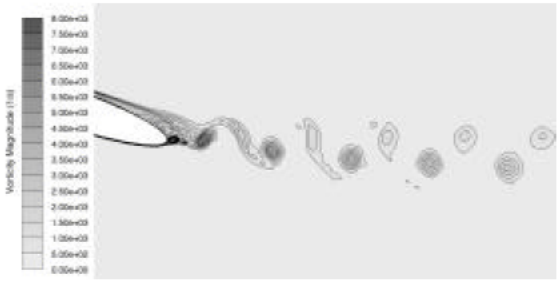

Fig. 10: Contours of instantaneous vorticity magnitude for DES model

calculations are consistent with a smaller effect of the separation compared to the DES runs. The success of DES at these angles of attack can be attributed to its LES treatment of separated region and wake zone, an outcome that contributed to improved predictions. Shown in Fig. 9 and 10 are contours of the instantaneous vorticity magnitude near the trailing edge and in the wake for RANS and DES predictions at 18.45° angle of attack corresponding to maximum experimental value of lift coefficient.

In Fig. 9 the S-A result shows relatively short shear layers that are diffused in the near wake. While the DES solution exhibits a typical wake structure dominated by the Von Karman streets and appears to posses some eddy content near the trailing edge. A regular modulation of the force coefficients was established that indicates a periodic shedding of vortices. The Strouhal number (St) based on a length scale defined as the vertical distance between points of mean separation at the trailing edge (Paterson and Baker, 2004) is equal to 0.25. This value corresponds to Strouhal number for flow over circular cylinder at the same Reynolds number. DES approach predicts a stall at 24.15° angle of attack, this is largely superior to the experimental value and the predicted values of C_l and C_d are still far from the experimental results. Also we can note that some tests with two different values of C_{DES} (0.25 and 0.85) have been carried out but poor predictions was found with incorrect values of lift and drag coefficients.

CONCLUSIONS

DES computations of the flow around elliptic airfoil were performed using a hybrid grid. Lift and drag coefficients were computed at various angle of attack and compared to experimental values and to those from S-A predictions. The accuracy of DES predictions is superior to that of Spallart-Allmaras model and the computed values of C_l and C_d are in good agreement with experimental results up to stall point. The complex shedding process and modulation in the forces appear to be represented reasonably adequately at least in relation to the agreement between simulation and available experimental results. Prediction of separation point at stall continues to strongly challenge current DES modeling approach, this 2D DES study fails to predict the stall for this configuration of flow. The RANS zone size influences substantially the overall accuracy of DES predictions. Overall, the results are encouraging, in order to continue investigating the DES approach.

REFERENCES

Benazza, A., E. Blanco, J. Parrondo and J. Fernández, 2005. Turbulence models in symmetric airfoil simulation, In: Proceedings of the 1st international congress of energy and environment engineering and management, May 18-20, 2005, Portalegre, Portugal.

Constantinescu, G., R. Pacheco and K.D. Squires, 2002. Detached-Eddy Simulation of flow over a sphere, AIAA Paper 2002-0425.

Kotapati-Apparao, R.B., K.D. Squires and J.R. Forsythe, 2004. Prediction of the flow overran airfoil at maximum lift. AIAA paper 2004-0259.

Lugt, H.J. and H.J. Haussling, 1974. J. Fluid Mech., 65: 771.

Mittal, R. and S. Balanchadar, 1996. Direct numerical simulation of flow past elliptic cylinders. J. Comp. Phys., 124: 351-367.

Nikitin, N.V., F. Nicoud, B. Wasistho, K.D. Squires and P.R. Spalart, 2000. An approach to wall modeling in Large-Eddy Simulations. Phys. Fluids, 12: 7-10.

Paterson, E.G. and W.J. Baker, 2004. Simulation of steady circulation control for marine-vehicle control surfaces. AIAA Paper 2004-0748.

Rhie, C.M. and W.L. Chow, 1983. Numerical study of turbulent flow past an airfoil with trailing edge separation. AIAA J., 21: 1525-1532.

Spalart, P.R. and S.R. Allmaras, 1994. A one-equation turbulence model for aerodynamic flows, La Recherche Aerospatiale, 1: 5-21.

Spallart, P.R., W.H. Jou, M. Strelets and S.R. Allmaras, 1997. Comments on the Feasibility of LES for Wings and on a Hybrid RANS/LES Approach, Advances in DNS/LES, 1st AFOSR Int. Conf. on DNS/LES, AUG. 4-8, 1997, Gredyen Press, Columbus Oh.

Spalart, P.R., 2001. Young person's guide to detached-eddy simulation grids. NASA CR-2001-211032.

Travin, A., M. Shur, M. Strelets and P.R. Spallart, 2000. Detached-eddy simulation past a circular cylinder, flow. Turbulence and Combustion, 63: 293-313.

Viswanathan, A., K.D. Squires and J.R. Forsythe, 2003. Detached-Eddy simulation around fore-body at high angle of attack, AIAA Paper 2003-0263.

William, D.H. and A.F. Brown, 1937. Experiments on an elliptic cylinder in the compressed air tunnel. RM N. 1817, British A.R.C.